INSTRUMENT- MOUNTED PRESSURE-SENSING SYSTEM FOR SURGICAL APPLICATIONS

A THESIS SUBMITTED TO THE GRADUATE DIVISON OF THE
UNIVERSITY OF HAWAII IN PARTIAL FULFILLMENT
OF THE REQUIREMENTS FOR THE DEGREE OF

MASTER OF SCIENCE

IN

ELECTRICAL ENGINEERING

AUGUST 2017

By
Isaac Kaleonahenahe Lum

Thesis Committee:

Aaron T. Ohta, Chairperson
Olga Boric-Lubecke
Galen Sasaki

In Collaboration With:

Dr. Maurice Garcia M.D

Abstract

Pressurized liquid may be utilized during an operation to inflate or clean a bodily cavity. If high pressures are sustained within the body, bodily injury may occur. This thesis discusses a system designed for physicians for monitoring internal fluid pressures as a physiological measurement. The pressure data is taken though a disposable, instrument-mounted, piezoresistive FlexiForce sensor, and measurements are displayed to the physician in real-time. The physician can then opt to receive alerts when an excessive pressure has been reached, to help avoid post-surgical complications. A linear pressure-voltage calibration procedure was developed using carefully measured deadweights, and a liquid-environment simulation device. Repeatability, hysteresis, reproducibility, linearity, and temperature-dependency tests were performed to characterize performance and determine the viability of such a system. The system was determined to be a good candidate for further experimentation, with a typical measurement error of ± 4.5%.

CONTENTS

i. List of Figures

ii. List of Tables

1. Introduction

1.1 Introduction

For centuries, surgeries have been messy affairs using crude instruments without precision or sensory feedback for minimal invasiveness [1,2]. While the medical field has since progressed, other sciences such as biology, chemistry and physics, had seemingly surpassed the medical findings in terms of innovation [3]. As the technology advanced the disciplines joined forces to bolster the medicine of the day. Biologists and chemists helped develop new medicines and antibiotics, while engineers focused attention on instruments such as the electrocardiograph or x-ray machine [4,5]. Now, with the help of machines, physicians can now literally see into the body [6]. Instruments have been engineered to allow a physician to enter the body, and perform an operation with minimal trauma and a high recovery rate [7]. In the hands of a skilled surgeon, these bio-instruments can be a great tool to diagnose and treat disease, but even these are limited to the surgeon's sensory abilities. In such a complex and fragile environment as the interior of the human body, even the sharpest of senses cannot always be used for navigation. When physical senses are not a viable option, the physician must often rely on device feedback to provide them with the sensory input needed to perform a successful operation. These *sensors* provide a means of measuring some biological variable. A sensor can provide much deeper, more precise, and more accurate understanding of physical phenomena within the body, as well as transduce physiological variables into a form much easier to interpret. For example, a biopsy procedure may require an internal tissue sample. While it may be possible to collect the sample using a needle probe, an

endoscope with a sensor in the form of a high-definition camera could collect the sample much more precisely, and minimize patient injury [7, 8].

1.2 Specialized Pressure Sensors for Surgical Applications

Sensors have pervaded nearly every facet of technological applications, and medical equipment is no exception. These sensors come in a wide variety of shapes, sizes, and functions, each tailored to best suit its application. The medical field presents interesting design constraints to an engineer, especially to those designing devices for use within the human body [9]. In addition to sensor performance, the engineer must take into consideration a litany of other important parameters. Sensors intended for use *in vivo* (in the living body of a plant or organism [10]) must be biocompatible, so that they do not expose internal tissues to toxic materials. Perhaps even more challenging are the tight space constraints. Incisions created during surgery must be as small as possible to minimize collateral damage and reduce recovery time [11]. When using an instrument such as an endoscope or laparoscope, on-board instruments are designed such that all needed tools are able to fit neatly into an incision as small as 1 to 2 cm [12][13]. Fortunately, some sensors can fit these size criteria [14][15][16][17]. Each of these bio-sensors plays an important role in the study of the human body. The data gathered from these devices are potentially lifesaving.

In a delicate and intricate environment like human body, medical instrumentation usually must rely on a combination of sensors, transducers, and electrodes to serve as surrogate eyes and ears to the operating physician. Some instruments are fitted with cameras to relay a live visual feed back to the physician, while other non-visible

measurements such as temperature, pressure, or chemical composition must be taken in juxtaposition with optical feedback [18][19] While not as visually obvious as the camera feed, these other physiological parameters play just as vital a role in the success of an operation.

Endoscopic, laparoscopic, and robotic operations have become increasingly more common, as they decrease recovery times, operation lengths, and pain, as well as cut down on the number of risks and complications [20][21][22][31]. While it is true that these instruments do help overcome some of the shortcomings associated with direct human error, machines lack the tactile feel of the human hand [13][21]. As far as sensor technology has progressed, the precision haptic feedback offered by the human hand for certain applications, has yet to be matched [21][22][23]. Despite this, mechanical and electrical sensors are still of great use, as the human hand cannot accurately discern force related input such as minute changes in pressure. For now, the best solution for this conundrum is to outfit the instrumentation with as many force sensors as possible to compliment and work in conjunction with the physician's own tactile feedback. Robotic systems such as the da Vinci system do have complex force and pressure feedback systems [24][25], and yet many surgeons opt not to use it due to high costs, and the lack of the full range of laparoscopic instruments [25][26][27]. This leaves surgeons with instruments that can perform specialized tasks, yet do not provide pressure-tracking capabilities. This parameter is particularly important in fields such as cardiology and urology, where liquid pressures are utilized [28][29][30].

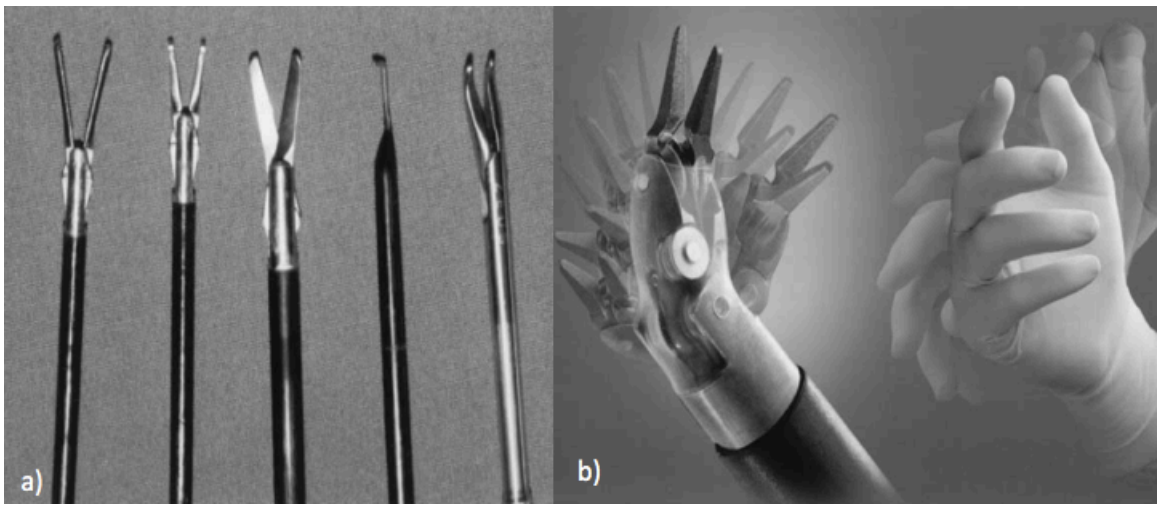

Figure 1: a) A variety of 5mm attachments for laparoscopic surgical instruments (figure from ref. [35]). b) An 8mm robotic wrist attachment for the da Vinci robotic surgery system. The attachment provides articulation simulating that of a human wrist, but does not come equipped with distal force sensors (figure from ref. [34]).

The problem of accurate pressure measurements in very tight spaces is further compounded by the rigid mechanical nature of conventional sensors. There has been a marked paradigm shift towards highly articulated and flexible robotic instrumentation [25][31][32][33]. The instrumentation is often steered through tortuous cavities, to access the operation site. Equipment must be robust enough to withstand stress inflicted by steering movements, and have minimal spatial impact [25]. Thus, any sensing instrumentation, whether built in or attached, should also adhere to the flexibility of steering mechanism.

Not all minimally invasive surgical equipment comes with pre-installed pressure sensors [21]. Because of this, the physician may not always track internal pressures, despite the use of pressurized fluids [28][30]. This also stems from the fact that tools and sensors are often inserted in the hollow body of the guide instrument, and all available internal space may already be taken to accommodate tissue manipulation end effectors. A

potential solution to this problem is to provide an externally mounted sensing system. This could potentially provide a means of pressure detection for systems that are not already equipped with such, or those that do not have the internal spatial capacity to accommodate. The focus of this paper is to provide a low cost, instrument-mounted liquid-pressure sensor for surgical applications, especially minimally invasive operations.

The intended applications and demonstration of usefulness will be discussed in Chapter 1. Design and construction of the device and all necessary components will be detailed in Chapter 2. Testing and calibration to characterize performance and determine the viability the system are detailed in Chapter 3.

1.3. Surgical Applications

Often in urological examinations or procedures, the bladder must be inspected. Usually this is accomplished with the aid of instrumentation inserted into the urethra or an incision in the abdomen. To aid inspection, the bladder can be filled with liquid, and a light source attached to the tip of the instrument illuminates the cavity. The liquid flow can be continuous, with water constantly entering and exiting the cavity, or single ended, with the pressurized liquid being pumped in and sealed [35][36][42].

The need for a highly specialized sensing system can be highlighted in one particular operation. Bladder Suspension Surgery is a form of abdominal surgery, used to treat stress incontinence in females [35][37]. Stress incontinence is the involuntary loss of urine due to some manner of physical stress or strain on the body. This can include coughing, sneezing, laughing, hiccups, or heavy lifting. When strain from physical activity is applied to the body, the pressure within the abdomen increases, and can press

on the bladder. Normally, the pelvic muscles are strong enough to withstand the added forces, however a damaged or weak tissue can cause urine to leak out by forcing the urethra open. While this is more frequently an issue with women over 40 [38], the damage to ligaments anchoring the uterus and bladder to the pelvic bones during childbirth can also cause incontinence. Up to 40% of women in their late fifties will have urgency problems, and of those, 40% may also develop incontinence [39][40].

This condition can be corrected or alleviated by bladderneck suspension surgery. This procedure can be performed though both open surgery or laparoscopically, employing a technique known as Burch Colposuspension [41]. In the open surgery, an incision is made in the abdomen, and in indwelling catheter is inserted in to the urethra. To assist in the identification of the bladderneck, the bladder may be partially filled with liquid or CO_2.

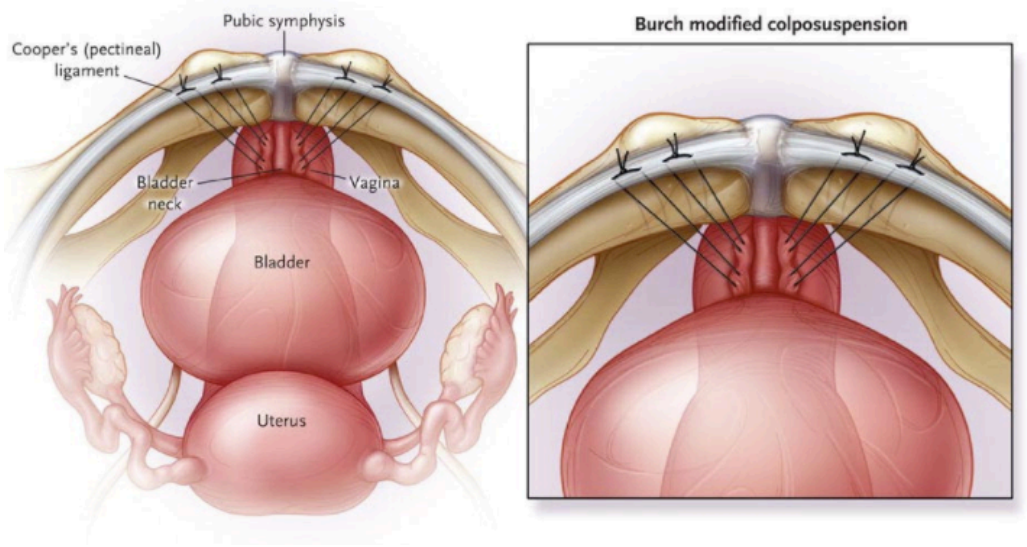

Figure 2: Bladderneck suspension surgery for urinary incontinence. This operation involves attaching the neck of the bladder to the back of the pubic bone using a technique called Burch Colposuspension (figure from ref. [41]).

Over-inflation of the bladder due to high liquid pressures during surgery can lead to complications. In the event of high pressure in the cavity, tissue damage can occur. This can cause the bladder to enter a state of paralysis [42]. During this period, the patient may experience abdominal pain, and an inability to urinate without the need for a catheter. Eventually the bladder will return to its normal state, however it is hypothesized that it is possible to avoid this complication through careful scrutiny of pressures via specialized instrumentation.

Due to the complications associated with excessive pressures within the bladder, it is important to monitor conditions throughout the operation. An analogous example to this proposed system is electrocardiograpy or electroencephalography. These methods include the placement of sensors to monitor physiological changes. The data gathered from running these tests can then be analyzed to reveal physiological trends that have a known correlation to certain conditions. Diagnosis is much easier, and may also lead to predictions so the preventative measures can be taken. Although an instrument-mounted device has not yet been implemented for the *in vivo* measurement of liquid pressure, it could prove useful in the prediction of post-procedural complications [43][44].

2 . Instrument-Mounted Pressure-Sensing System.

2.1 System Overview

The Instrument-Mounted Pressure-Sensor System is a prototype intended to collect real-time data for physicians performing any surgery that requires close scrutiny of liquid or ambient pressure. The device will be used to gather enough data to analyze and determine an optimal pressure range during a procedure. Currently, the operations are performed without the collection of water pressure data, and the correlation between the pressure conditions maintained in the bladder and complication rate has not been thoroughly studied. With this system, the physician can track the pressure in real-time, and receive an alert if an unsafe pressure has been reached.

The data collected during the surgery is to be analyzed alongside surgical results, as well as post-surgical follow up visits by the patient. Careful examination of the pressures sustained during the operation can then reveal trends that relate the pressures that the bladder is exposed to during operation, to the surgical success rate and recovery time. This can lead to the formation of a standard pressure range to be maintained to provide optimal results.

The system consists of three segments, a thin pressure sensor, a data acquisition unit, and a visual computer interface.

2.2 Components

2.2.1 Instrument Mounted Pressure Sensor

The focal point of this system is a thin flexible pressure sensor to be mounted to the exterior of an instrument. While pressure sensors are not a particularly new technology, the placement and operating environment of this device adds a new dimension of physical constraints to the design. In addition to performance optimization, the system must also be compatible with use in the body. This includes the use of non-toxic materials, and constraints on the sensor geometries to provide the patient with maximum comfort. As previously discussed, surgical instruments operate in confined spaces, and not all instruments come equipped with pressure sensing capabilities. Steering and actuation mechanisms occupy the entirety of the instrument interior, leaving little space for added instrumentation such as sensors. Thus, point-of-contact sensors are less common. To solve this problem, a mounted pressure sensor was tested. This confers pressure-sensing capabilities to a system that is not already equipped with built-in pressure sensors, with minimal modification.

The sensor is connected to a data acquisition unit, allowing the system to acquire data *in vitro* during the operation. The sensor is removable, and ideally disposable, so as to eliminate cross-contamination between patients.

Figure 3: Karl Storz 2470 SL rotating continuous flow sheath. The sensing apparatus can be affixed to the end of a device like this, which is then inserted into the patient's urethra.

There are certain important characteristics for this sensor. In addition to performance, there are certain physical attributes to consider. These attributes include:

Thin Profile: The sensor will be mounted to the exterior of an instrument, and may be in direct contact with tissue. One of the advantages that minimally invasive surgeries offer is their small incision sizes. This is mainly due to the minimal size of the instrumentation [20], and anything mounted to the exterior of the instrument should have a very low profile to reduce risk of tissue abrasions. Because of this, it is imperative that the sensor be as thin as possible, with a smooth outer surface. This will help minimize the friction and possible abrasions due to irregularities on the otherwise smooth surface of the instrument. Thus, the sensor is to be less than 0.3 mm in thickness.

Flexibility: The sensor must conform to the shape of the instrument. The flow sheath shown in Fig. 3 is rigid, although some of the surgical devices could be flexible, such as a catheter. The sensor must be able to conform to the shape of the device, without

perforating or losing adhesion. While maintaining contact with the instrument, the length of the sensor must also accommodate the movements of articulation, including steering and actuation. The construction material must be robust enough to tolerate the mechanical strain induced by bending and twisting, and yet flexible enough not to hinder these movements.

Waterproofing: The instrument will be exposed to bodily fluids, and often submerged in liquid, so it must be able to prevent water leakage into the electrically sensitive components.

Secure: This system is intended for integration with a wide range of cylindrical instruments, so the sensor fastening mechanism must require as little instrumental modifications as possible. The sensor must be easily mountable and removable while still providing structural integrity during steering and actuation motions. It must also be placed in such a manner as not to obstruct instrument articulation. The sensor also should not dislodge during operation, even if it is in contact with tissues. Due to the highly sensitive nature of the sensor material, improper mounting could interfere with calibration, and affect the accuracy of pressure measurements.

Disposability: The sensor itself is ideally disposable in order to prevent cross-contamination between patients. Thus, the sensor should be cost-effective enough to make this feasible.

Bio-compatibility: Construction materials must be non-toxic. This includes, but is not limited to, the piezoelectric or piezoresistive materials, capacitive dielectrics, encasing materials, adhesives, and sealants.

For testing and development purposes, a commercially available piezoresistive sensor was selected for the first prototype of the sensing system. The sensor was to have the key qualities mentioned above, in addition to high performance in the expected operation range of less than 1 N of applied force.

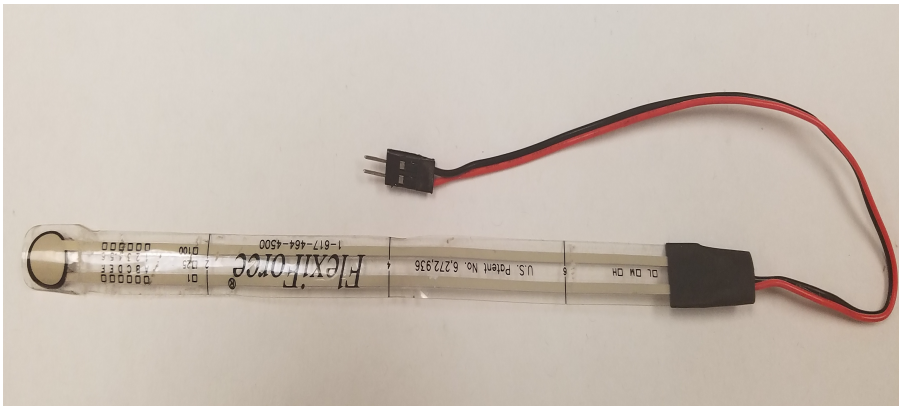

Figure 4: Flexiforce A201 piezoresistive sensor. This water resistant, flexible sensor has a range of 0 - 4.4N [45]

The sensor selected was the Tekscan Flexiforce A201 piezoresistive sensor, chosen for its flexibility and ultra-thin profile (Fig. 4). This sensor was employed for initial baseline testing, as well as to develop testing and calibration procedures. The polyester construction provided a degree of water resistance, however the sensor was further waterproofed to prevent short circuits due to water leakage.

Table 1: Flexiforce A201 piezoresistive sensor physical properties [45]

Flexiforce A201 Sensor Property	Value
Thickness	0.208 mm
Width	14 mm
Length	152 mm
Sensing Area	9.53 mm
Substrate	Polyester
Force Range	0-1 lb
Response Time	< 5 µs
Operating Temperature	-9˚C - 60˚C

Thin- film piezoresistive sensors such as the FlexiForce are a particularly appealing option for this application. Piezoresistive sensors have been often used to take reliable force and pressure measurements in biomedical applications [46][47]. Most often constructed from pressure-sensitive ink between flexible polymer sheets, piezoresistive sensors are favored for their straightforward operation and read-out technique [48]. Other sensing options do exist, such as capacitive and optical pressure sensors. Capacitive pressure sensors are highly scalable, and do offer some performance advantages over their piezoresistive counterparts. By comparison, capacitive sensors have a higher sensitivity, lower power consumption, and less drift [48][49]. However the complexity of the required capacitance sensing circuit, and potential signal loss from parasitic capacitances [49][50] made this sensor type less appealing for initial system prototypes. This prototype will seek to eliminate some of the potential electronic

packaging errors to focus on proving the viability of the system. Once operation has been established, the higher sensitivity of the capacitive sensor can be explored. Optical pressure sensors use light to measure pressure-induced deflections in a flexible diaphragm. Though highly sensitive, they require complex calibration and optical alignment, and are highly temperature sensitive [51]. In addition, commercially available options were too large for this application, and were thus not considered.

Several manufacturers besides Tekscan do produce thin-film piezoresistive sensors. Sensors by LuSense and Interlink have comparable construction and performance. All have a polyester construction with a circular sensing area, and similar sensing ranges. The LuSense and Interlink sensors have a more robust construction and slightly quicker response time. However, the Tekscan Flexiforce sensor was shown to have the best precision, linearity, and repeatability [52].

FlexiForce sensors have also been preferred for use in biomedical applications, for reasons mentioned above, as well as their thinner width. These sensors have been utilized in minimally invasive surgery to provide haptic feedback for the Da Vinci robotically assisted surgical system [53], as well as the mapping of foot pressure to predict diabetic ulceration [54]. Applications such as monitoring of extraocular compression during craniotomy [55], and tissue characterization during cardiac surgery [56] provide greater precedence for *in vivo* usage over other manufacturers.

The Flexiforce sensors, while flexible, are inherently flat. The sensors required a modification to allow the sensor to adhere to the curved surface of the mounting instrument. This proved challenging for several reasons. The instrumentation to which the sensor is to be mounted ranges in diameter from 24 French (Fr) to 26 Fr (8 mm to

8.67 mm), and the sensor must tightly fit to the surface of the instrument without impacting the performance characteristics of the piezoelectric substrate too severely. The first attempts at achieving this involved the used of a double-sided adhesive tape, fitted to the underside of the sensor. This proved unsatisfactory, as the adhesive did not provide sufficient strength to counteract the outward flexing of the edges of the sensor. Due to the stiffness of the sensor, the edges around the sensor head had a tendency to peel off, posing an abrasion risk. Although perhaps a stronger adhesive tape could be used, the sensor should also be easily removable by the physician. A very strong adhesive tape or glue is not easily removable and may leave behind residue. This issue was resolved by the modification of the sensor to maintain a curved surface. This was difficult, as any sharp bends in the piezoelectric material severely damages the sensitivity [57]. The active sensing area is constructed of a layer of piezoresistive ink between two layers of silver. Any deformations or stress to and around the sensing area that alter its original resting state will cause resistance to decrease. Thus, simply forcing the sensor into a cylindrical shape from a flat rest state will negatively affect the sensitivity by decreasing the resistance range. To combat this, a curvature was introduced into the sensing area to keep the resting state resistance high. The sensor was tightly wound around a 6-mm-diameter steel rod and heated to 87˚ for 2 minutes. This process allowed the polyester to soften and curve, while preventing any creases or perforations. Once cooled, the sensor maintained its curvature. The resting-state resistance remained in the range of 5 to 10 MΩ, similar to unaltered sensors.

Although this particular sensor is a good fit for prototyping and testing, it still required modifications to adhere to all the requirements of this application. As previously

mentioned, the sensor was water resistant, but not fully waterproofed. Splashing and momentary wetting was found to have no significant impact on performance, however full immersion in liquid has noticeable effects. Over time, moisture wicked between the lamination glue of the polyester construction, leading to short circuits and erroneous data. For the target application, the sensor is to be fully immersed in liquid and pressurized, therefore waterproofing is imperative. To accomplish this, the edges of the sensor were coated with a thin layer of silicon adhesive. As the polyester layers comprising the top and bottom of the sensor are waterproof, only the edges required additional moisture prevention. Though this method provides complete waterproofing, it was not a practical solution. Silicone adhesive requires extensive curing times, and can be difficult to remove. A much quicker solution to this issue is to enclose the sensor in a watertight sleeve made from single and double-sided polyimide tape. A layer of single-sided polyimide tape with a thickness of 80 μm was placed over the active sensing side of the sensor, and a double-sided layer polyimide tape of the same thickness was bonded to the single-sided tape, around the sides of the sensor as shown in Fig. 5. The excess tape is trimmed from the outer sensor edges, leaving several millimeters of bonded polyimide around the sensor edges to prevent leakage. The bottom polyimide layer also serves as a strong bonding agent to the instrument surface, providing a waterproofing and mounting mechanism with minimal added thickness. The polyimide surface is smooth, so the risk of detachment due to snagging an edge is low. A sensor waterproofed in this manner was left submerged for 24 hours in dyed water. When removed, the sensor remained in proper working order, and no evidence of moisture penetration between the adhesive was found.

Figure 5: Waterproofed Sensor. Polyimide tape bonds around the sensor to for a waterproof lamination sleeve.

With the curvature modifications discussed earlier, the adhesion strength of the polyimide tape is sufficient to prevent lifting of the edges of the sensor. This method allows for a simple application of the sensor by the physician to the instrument, and leaves behind no residue.

Although initial testing was performed using a piezoresistive sensing mechanism, alternative measurement options will be explored in later sections.

2.2.2 Data Acquisition Module

The second component in the system is the data acquisition module (DAM). This device contains all active electronics and circuitry (Fig. 6). The purpose of this component is to acquire data samples from the sensors, and convert the information to a digital format for analysis. After the sensor has been affixed to the surgical instrument, it is then connected to the input portal of the signal acquisition unit. The DAM provides

power to the sensor at the appropriate end, and receives feedback on the other, dependent on environmental conditions.

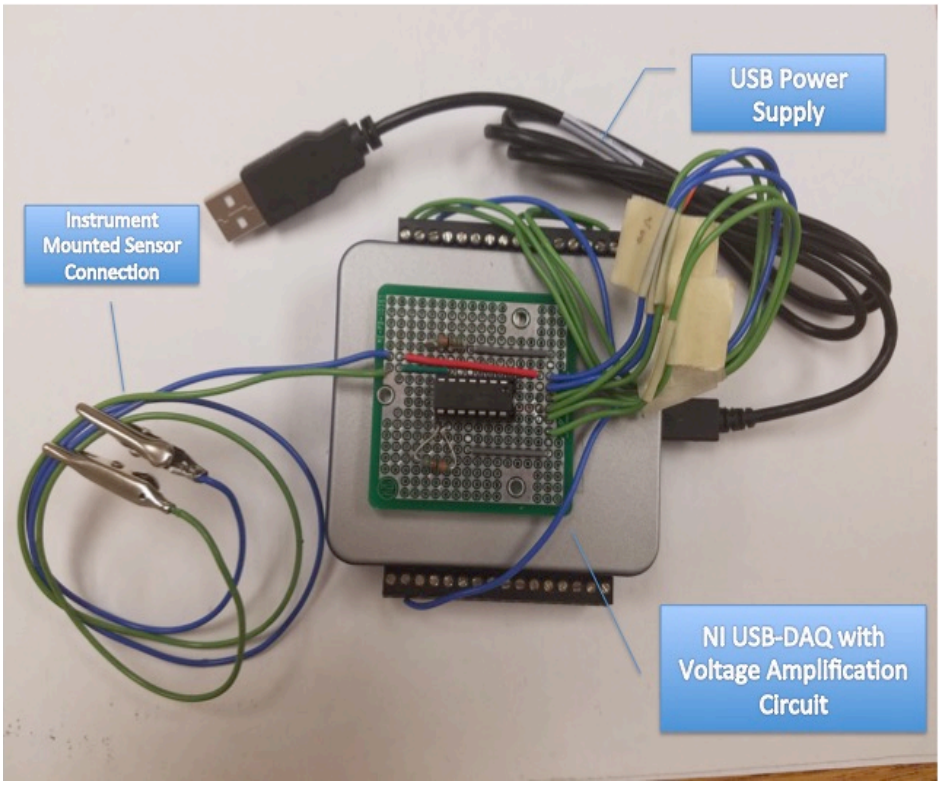

Figure 6 : Data acquisition module with USB power supply, amplification circuitry and alligator clip test connections.

The system consists of a primary data acquisition unit and various amplification and power circuitry. The live data acquisition is provided by a National Instruments USB Data Acquisition unit (DAQ). This device also supplies the amplification power, variable drive voltage, and common ground source.

The entire system is powered by via a USB terminal. The NI DAQ-USB6001 is equipped with two output channels with 10V maximum signal voltage capabilities. Input signals to the inverting terminal of the op-amp, in mV range, are amplified to 6 volts. The feedback resistor can be adjusted depending on desired sensitivity (Fig. 7). A large resistance value and a low drive voltage will prevent the op-amp from saturating at higher

pressures. For this application, a higher sensitivity at low-pressure ranges was desired, so the feedback resistance was set at 33 kΩ.

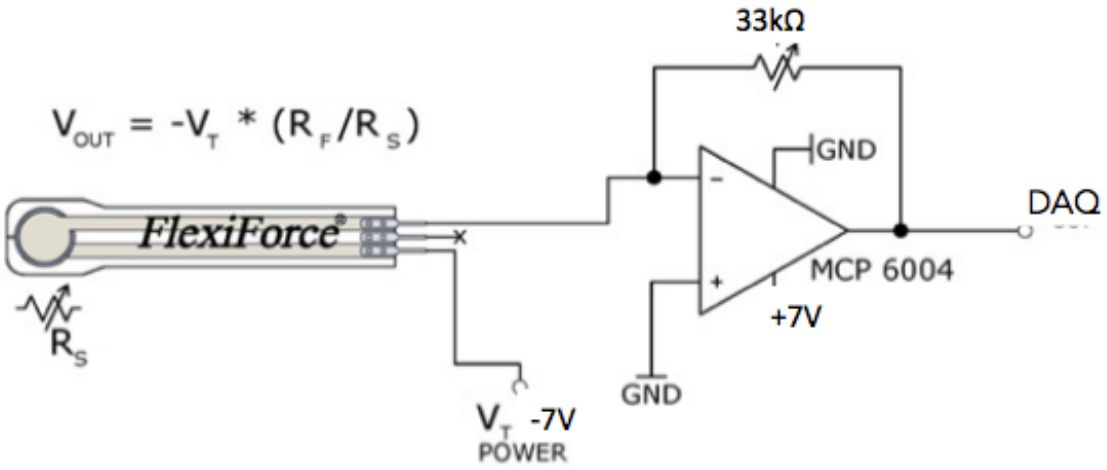

Figure 7: Piezoresistive sensor circuitry (figure from ref.[45])

Initial testing and calibration procedures were performed with piezoresistive sensors, compatible with the setup described in Fig. 7. However as other transducer options such as capacitive sensors are explored, this setup required modifications.

For experiments with capacitive type pressure sensors, a special conversion circuit was required. This particular NI-USB-DAQ, does not have direct capacitive sensing abilities. Input must be in the form of a voltage signal, and modifications were required to convert the changing capacitance into a form interpretable by the DAQ. With a resistive sensor setup, pressure is sensed by the DAQ by measuring the voltage changes due to the modified, strain-induced changes to the piezoresistive material. A DC drive signal, and an analog voltage sensing port are all that is needed to sense pressure. To allow the use of the same DAQ, an AC voltage output generation port was added to power the capacitive sensor. The applied force to the sensor causes a capacitive change, which is sent through

a frequency to voltage conversion circuit, repurposed to serve as a capacitance-to-voltage (CV) converter. There are several techniques of measuring capacitance, such as charge balancing or rise and fall time measurements, but this requires a complex electronics system and is not a cost-effective method for this prototype. A simple work-around for this problem is to use Texas Instrument's LM2917 frequency-to-voltage (FV) converter. The LM2917 is a monolithic FV converter with a high gain op-amp, to relay a load when frequency exceeds a selected rate [58]. However, its intended use has a non-linear characteristic curve, and is thus an unreliable method of recovering capacitance measurements.

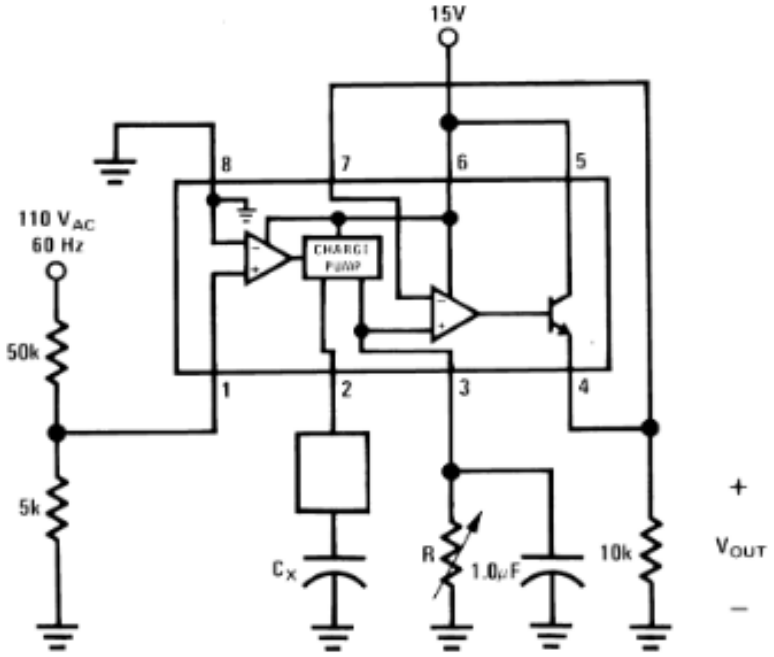

Figure 8: Capacitance to Voltage converter Circuit (Figure from ref. [58])

With a few simple changes to the port configuration, the LM2916 can be reconfigured to respond to capacitance changes directly (Fig. 8), and provide a highly linear relationship. Mathematically the output of the circuit is expressed by [59]:

$$V_{out} = F_{in} \times V_{cc} \times C_x \times R \qquad (1).$$

The output voltage is dependent on a frequency input F_{in}, the supply voltage V_{cc}, a capacitance value C_x, and resistance R. If the circuit is used as an FV converter, the supply voltage, capacitance, and resistance are all kept constant and the change in frequency determines the output. However, by fixing the supply frequency and varying capacitor C_x, we now have a linear output relationship between a voltage and varying capacitance. Although the LM2917 is capable of a supply voltage of up to 28V, this application is limited to the 10V power supply available to the DAQ.

The module is encased in a protective housing, to protect electrical components from possible liquid exposure. The structure consists of a cubic housing, fitted to the DAQ, with a snap-on cover. Entry ports are provided to accommodate the USB power connection, as well as the sensor connections.

2.2.3 User Interface

The most prominent feature of this system is the User Interface (UI). The UI enables the physician to interact with the system, control certain features, and receive feedback. The design of the interface was kept visually simple, so as to provide the physician with minimal distractions, as well as ease of operation. During surgery, it is important that the operating physician devote most of their attention to the patient. Therefore, it is critical that the live display of the data, be easy to interpret at a quick glance, and any warnings must be obvious at a quick glance.

Besides the graphical display of the incoming data, the interface must also record all samples, to be analyzed on the researching physicians' time. Because the surgery can last up to 3 hours, the collected data file size will be quite large, and will not be easily

interpolated by visual inspection. Data is must also be saved so that the time versus pressure curve can be reconstructed for inspection at a later time.

The GUI was created using LabView, a visual programming platform (Fig. 9). Although it is possible to access and control the DAQ using other programming languages, the recommended software was used to avoid compatibility issues and facilitate ease of programming.

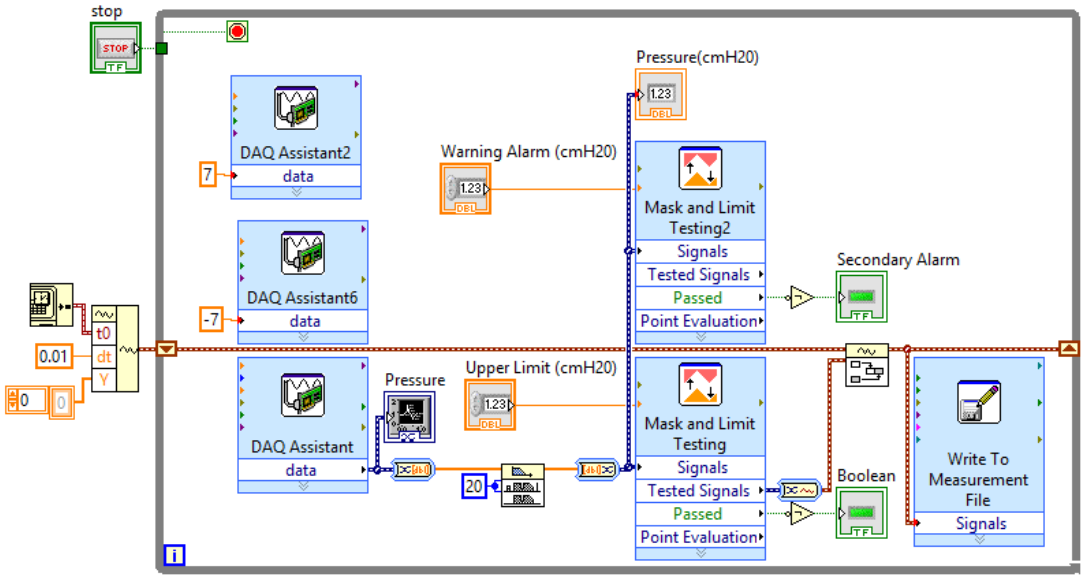

Figure 9: Real-time pressure feedback display programming block diagram. The DAQ is used to power all active IC's, and collect measurements for immediate display as well as storage.

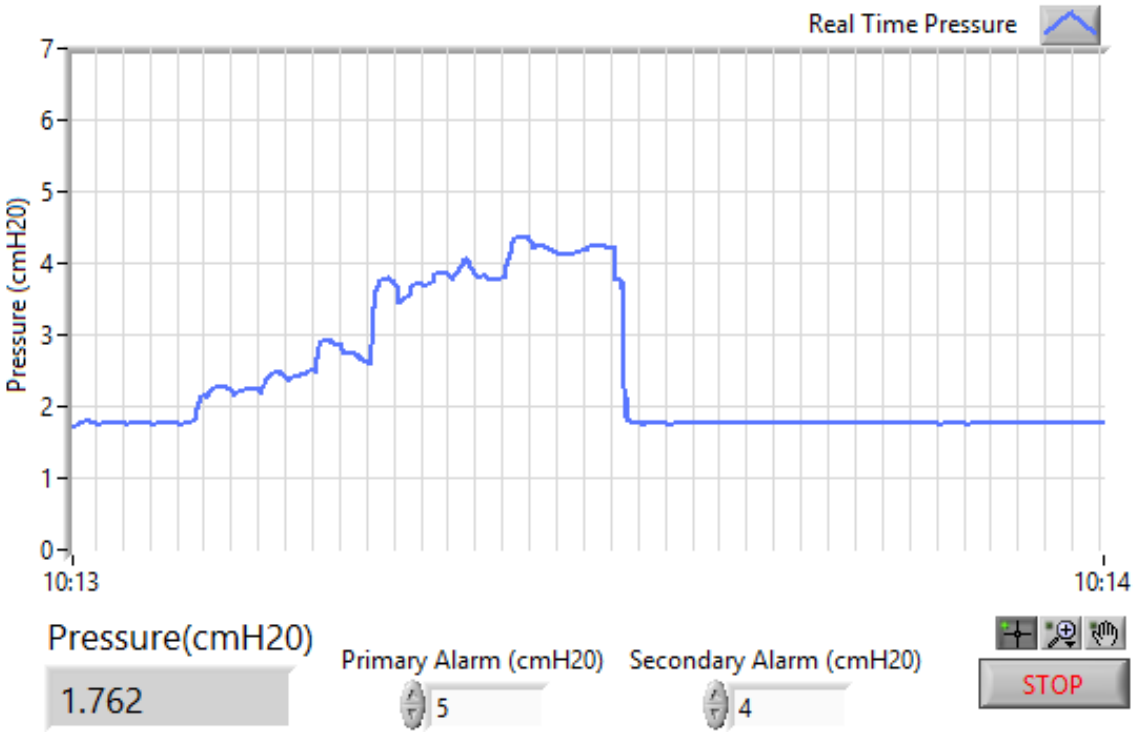

Figure 10 : Graphical User Interface created in LabView.

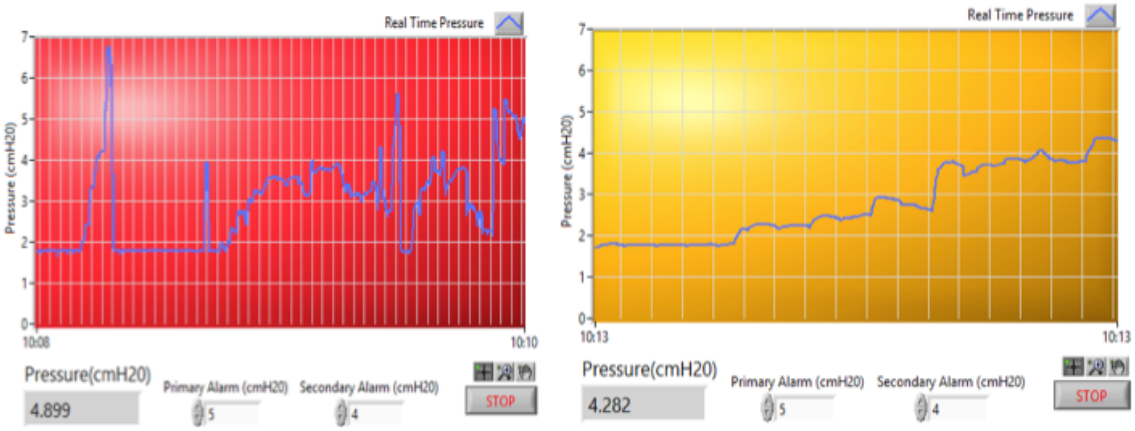

Figure 11: Primary and secondary alarm triggers

The appearance of the interface was kept simple, to minimize distractions to the attending physician. There are three key features for the physician. Firstly, a real-time

plot of the pressure vs. time is prominently displayed (Fig. 10). Values are appended to form a chart, so that the instantaneous pressure can be compared to previous values, and the physician can maintain a more constant pressure if desired. In addition to the graphical display, the numerical value of the instantaneous pressure is shown in units of centimeters of water (cmH_20). Secondly, the user is given a field in which to enter alarm trigger values. The value for the upper limit will trigger an alarm if the value is reached or surpassed. A secondary alarm value can also be set to notify the user that the pressure is approaching the upper limit. The alarms appear as color changes to the background of the pressure vs. time plot. A white background indicates a safe operation range, an orange background indicates that the secondary alarm has been triggered, and a red background indicates that an unsafe pressure level has been reached (Fig. 11).

Raw data from the output of the op-amp do show a fair amount of noise, especially at higher sample rates. To mitigate this, the sample rate was lowered from 100 Hz to 50 Hz, and noise reduction algorithms applied. At these low frequencies, the signal can be cleaned with a simple removal of large noise spikes, possibly caused by the steering of the instrument, and a focus on changes of baseline pressure levels [61][62]. A simple method of accomplishing this is to apply a moving median filter, a type of nonlinear filter often used in image processing to remove impulse characteristics [62][63]. This algorithm is used to help distinguish background noise drift from baseline voltage measurements while preserving points of interest. The median filter operates by filtering array X of size *n*, to an output array Y also of size *n*, with each element being a subset of points centered around the corresponding element. The size of the subset is dependent on

the selected rank r, where $n > r \geq 0$. The median of each subset is sorted and placed into output array Y, effectively removing all data points that compose less than 50% of a subset. This filter removes sharp peaks, with severity of segregation in favor of more even sections dependent on rank size. Smaller rank values tighten the subset filter window, and only allow the most acute excursions, while lower values will smoothen even the broadest peaks [64]. For this application, the median filter rank was set to 10.

The DAQ does not come with a built-in pressure-sensing meter. Raw analog data input is in the form of sampled voltages, and a correlation between the data type and expected output must be manually programmed. In this case, the relationship between the pressure and voltage should be ideally linear. This linear relationship must be experimentally determined, but once deciphered, can be imposed on all incoming voltage data. This way the graphically displayed data can be set to any unit type desired. A linear regression line of the form $y = mx + b$ is obtained via calibration. Incoming data x is multiplied by the slope of the best-fit line m, and added to voltage offset b, giving output y in the desired units (Fig. 12). The calibration process used to determine the linear fit will be discussed in a later section.

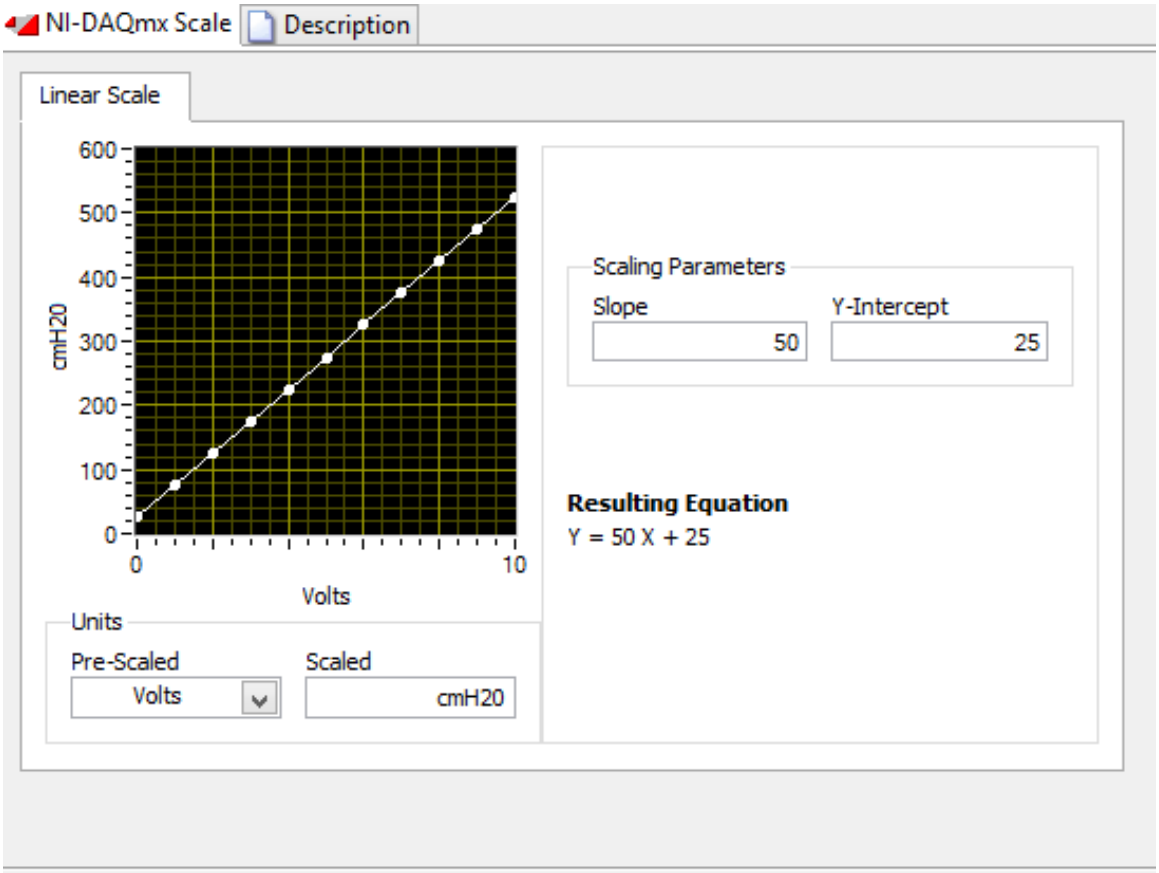

Figure 12: A Linear relationship between voltage and pressure can be established and imposed on collected data via software. The pressure conversion from voltage to cmH_20, is an equation in the form of y = mx +b.

The program was created in LabView, and converted into an application format, with an executable compatible with any Windows operation system. A LabView software license is not required to run the application.

2.2.4. Data Analysis Program

The final component to this system is a data analysis program to view data gathered during the operation. If a correlation between high pressure and the resulting medical complications are to be found, it is important to provide the tools needed for close

scrutiny of the data. Although the data is displayed continuously throughout the procedure, it may be difficult to process information while attention is needed elsewhere. In addition, the comparison of data gathered across multiple procedures performed by different physicians can shed light on important trends. As a result, a data analysis program was created to assist a researcher in interpreting data in a simple and comprehensive format.

The GUI has been programmed to record data points at a rate of 50Hz, and append them to a .csv (comma separated values) file, saved on the computer desktop. The saved file is then opened using a program, written in Python. The purpose of this program is to reconstruct the operation data, and assist the physician in identifying trends associated with over inflation damage. This is done by visual inspection of pressure/time curve of the entire duration of the operation. If the physician notices any unusually high-pressure peaks, it is possible to take the mean and median of a selected time frame. The mean, median, and peak over the entire duration is also calculated. From this, the physician can then begin to draw inferences, as well as pinpoint the exact time frame at which the damage is suspected to have occurred.

The program is written in Python a popular, high-level programming language. It was selected due to its functionality, pre-built packages, and ease of installation. Although LabView was used to create the GUI, and could have been used for analysis, expensive licenses may be required to run LabView. Python offers comparable functionality, but is free of charge.

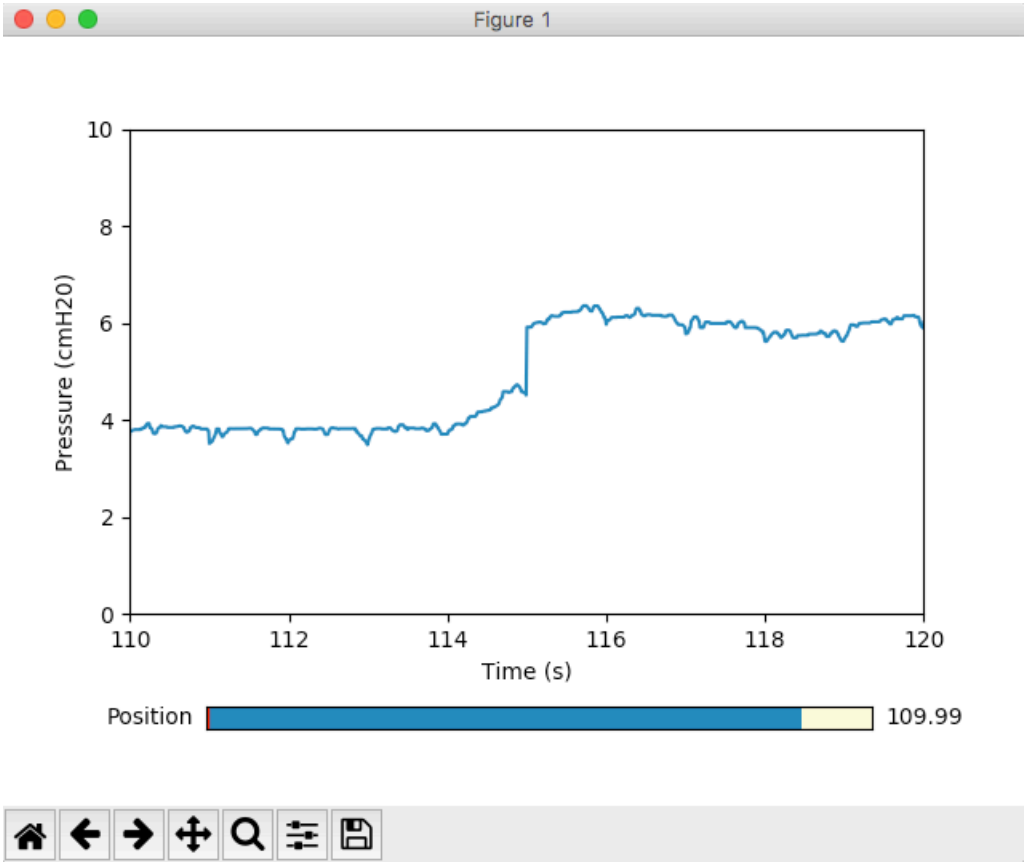

Figure 13: In-surgery pressure versus time curve. Reconstructed in Python using data collected in .csv format.

The program consists of a simple graphical interface, and several tools. Once the .csv file containing surgical pressure data has been obtained, the user is prompted by the program to enter the file path. The majority of the display window is a graphical reconstruction of the pressure (in cmH_20) versus time (in seconds) elapsed, shown in Fig. 13. The user is provided with a window of 100 s, and a scroll bar to navigate through sections of the curve. By moving the slider bar, the curve can be traversed over the entire duration of the operation. In this manner the physician can determine the times at which the cavity sustained the highest pressures. The physician can zoom in on an area of concern, and inspect the mean, median, and maximum pressure over that range. If the

physician wishes to examine a particular time range, a tool is provided to prompt the user to enter a time range, and the median, mean and maximum values are provided in numerical format.

3. Sensor Characterization

The pressure transducer must undergo rigorous testing to characterize its performance. For the sensor described in Section 2.2.1, its resistance varies with applied mechanical stress, but the relationship between the applied pressures and the resulting electrical output must be calibrated. This system employs an electrical transducer that is capable of converting mechanical input into an equivalent voltage. Whether the conversion mechanism is resistive or capacitive, the same calibration procedures can be applied.

Calibration is defined as the comparison of measurements against a known and accurate standard [65]. In this case, the measurement is the sensor voltage and the known standard is the applied pressure.

3.1. Testing procedures

To find the correlation between recorded voltage and pressure levels, a testing device was created. Initial testing of the piezoresistive sensors involved the careful placement of deadweights to act as known force values. The process begins with an object whose mass has been determined using a precision scale. Object mass can then be converted to a force using the well-known equation $F = m * a$, with a being the acceleration due to gravity, 9.8 m/s^2. Once the force associated with the mass has been obtained, we can then determine the amount of pressure it exerts over an area. Pressure is the amount of force applied over a certain area:

$$p = \frac{F}{A} \tag{2}$$

where p is the pressure in Pascals, F is the normal force in Newtons, and A is the contact surface area. The area of the Flexiforce piezoresistive sensor is 71.33 mm^2 [45]. If the entirely of the force is applied solely to the effective sensing area of the sensor, this formula can be used to relate a pressure measurement to voltage. A series of deadweights, each with increasing mass, were assembled and the forces were calculated. The masses were then individually applied to effective sensing area, and impedance of the sensor changes accordingly. The voltage shift due to the resistance modification was then recorded. The experiment can then be repeated until enough data has been gathered to construct a best-fit, linear relationship curve.

Initial testing and calibration using this method on a flat-surfaced transducer was fairly straightforward. A small disk, or "puck", was placed over the transducer, such that the entirety of the force was distributed evenly over the effective sensing area. During the calibration process, the entire sensing area is treated as a single contact point. Load forces must be evenly distributed across the sensing area to ensure repeatable measurements. A hollow plastic cylinder, 2.2 cm in diameter, was placed atop the weight distribution disk to hold weights (Fig. 14). Shifting of the load during the calibration can cause erroneous readings, thus a flat-surfaced loading platform such as a dish was abandoned in favor of a thinner cylindrical column. This made it easier to position the center of mass directly above the sensing area. Weights were added individually, and the total exerted force recorded. Water was used as the first weights, with liquid added in 5 g increments. Denser steel weights were then added until the column was full, and the desired pressure range was spanned. This method is more complicated when applied to a curved-surface transducer. To place the forces more evenly, a distribution device was fashioned from

rubber, and molded to fit the curvature of the effective sensing area when the sensor was mounted to the surgical instrument.

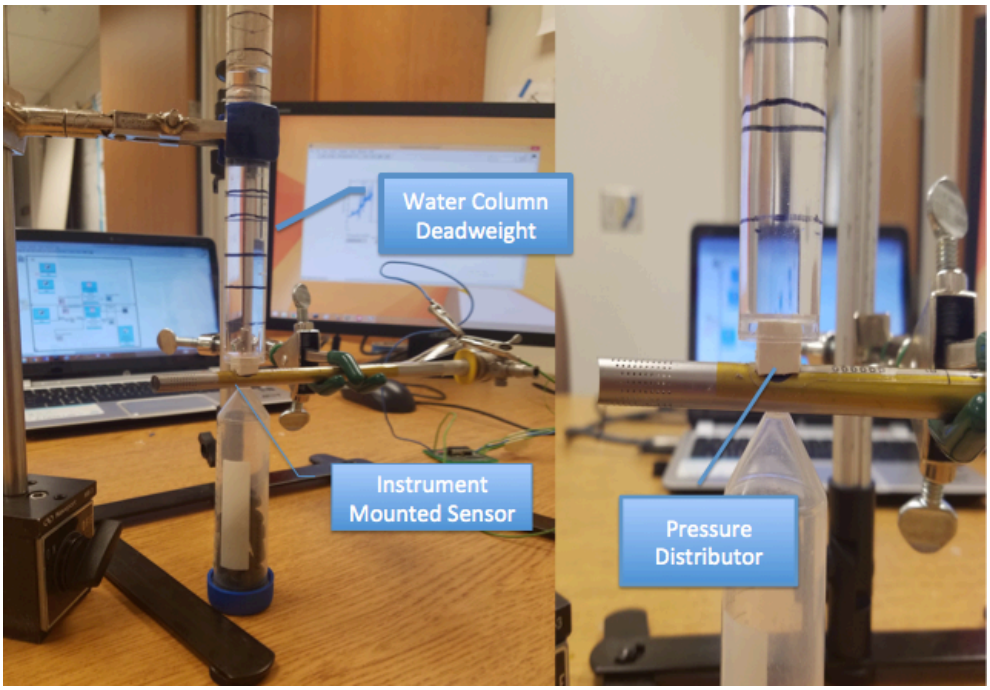

Figure 14: Calibration and testing procedure. A weighted column is placed on the sensing area, and corresponding voltages and forces recorded.

Although deadweight forces and ambient pressures are in this case equivalent, a second testing method was created to better emulate actual operation conditions. The units of measurement most commonly used by physicians are millimeters of liquid, usually water or mercury [66]. In this case, cmH_20 is the standard unit of measurement, and will be used as the unit of pressure for all experiments.

While deadweight testing is a convenient and accurate calibration method, a testing procedure more similar to the actual operation environment may be able to provide insight into system performance under liquid pressure. To this end, a liquid environment calibration device was also constructed. A 150-cm-tall water column was constructed

from clear vinyl tubing. The instrument-mounted sensor was placed through the bottom of the tube and sealed, such that the force exerted by the weight of the water column would bear directly down on the sensing area. Markings on the sides of the tube indicate the height of the water column in 0.5-cm increments. It is assumed that the only relevant mass is the tube is that of the column of water directly above the effective sensing area. The pressure exerted above this area can be found by first calculating mass of the water column using its volume and density. The relationship is:

$$m = \rho \times V \tag{3}$$

where the *m* is the mass in grams, ρ is the density of water (1 $\frac{g}{cm^3}$ [67]), and *V* is the volume of the cylinder of water. The volume of the cylinder is:

$$V = \pi \times r^2 \times h \tag{4}$$

The radius *r* in Eq. 4 is the radius of the sensing area (4.76 mm), and *h* is the height marked on the vinyl water column. Pressure can then be obtained using equation 2. Water was added from the top of the tube, and released into a drainage pan from a bottom valve (Fig. 15). This testing method also allows for temperature-varying experiments, as the added water can be heated to a specific temperature.

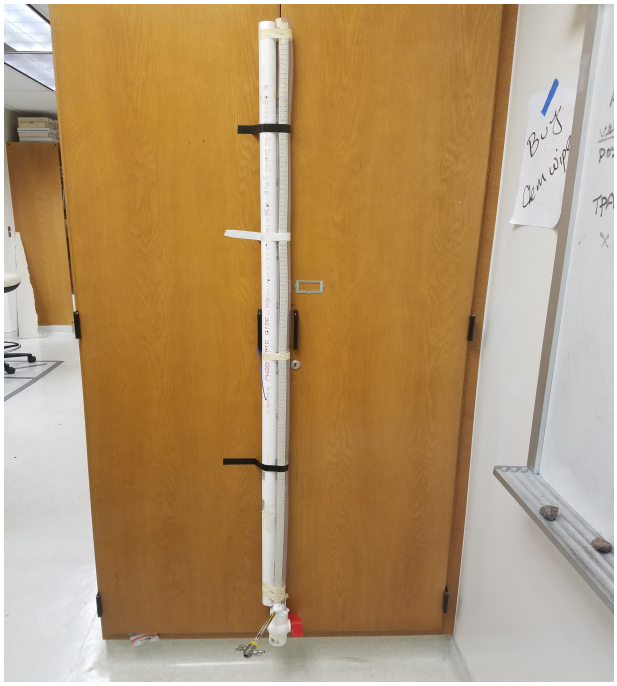

Figure 15: Water column test environment. A clear vinyl tube is affixed to a PVC pipe for structural support. The instrument-mounted sensor is inserted into the bottom of the tube and sealed. Liquid can be added to the top of the tube, and drained from a release valve at the bottom.

3.2. Performance Characterization

The system performance must be characterized before it can be reliably used to measure pressure. The characterization experiments are designed to test the performance limits of the sensor, and highlight some of the positive attributes. Performance characterization was also done to develop a simple and reliable calibration procedure. The characteristics tested are as follows:

Repeatability: Repeatability is defined as the deviation of the same measurements taken over a short time interval on a single sensor. This will test the agreement between successive readings, and measure the variance between output data when taking the same measurements [68].

Reproducibility: This metric will determine the variation of readings from sensor to sensor.

Accuracy: A measure of accuracy is the highest percentage deviation from an ideal value, after calibration [68][69]. The *error* is defined as the percentage inverse of the accuracy.

Sensitivity: Sensitivity is defined as the voltage change per unit of pressure applied. This change is ideally linear.

Linearity: The transfer function of the sensor is ideally linear, and non-linearity will be quantified as the standard deviation from the linear regression line over the full scale.

Hysteresis: Error induced by constant loading and unloading or wear.

Full Scale Output (FSO): The difference in voltage output between full input stimulus and lowest applied load.

Experimental data was tabulated in Excel and exported as a .csv file for processing. Data processing is performed in Python, using NumPy, a fundamental package for scientific computing in Python [70]. Graphical representations and plotting are also done in Python, using the 2D plotting library Matplotlib.

3.2.1. Operating range

This piezoresistive sensor has a wide operation range, up to 4 N. Obviously this range is not needed for biomedical applications, and electronic equipment has been tailored to optimize the sensitivity for much smaller loads. The liquid pressure range to be detected is 0 to 14.7 kPa, with forces less than 1 N, or 0 to 150 cm$H_2$0. The corresponding voltage

range is limited by the amplification circuitry to 0 to 6 V. Though the dynamic range of the sensor is much larger, pressure greater than this would not be feasible for any human operation, and will thus be omitted. The excitation voltage and feedback resistance have both been optimized to deliver the greatest sensitivity and FSO over this range.

Other factors can affect the operating range of the sensor. The unloaded sensor ideally has a very high resistance, in the range of 10 MΩ. As a force is applied to the piezoresistive material, the resistance should decrease accordingly. However damage to the sensing area, creases, folds, and even slight bends can lower the initial resistance and thus the range. A severe deformation, such as a sharp crease, can cause the resistance to drop drastically (to less than 1kΩ). This effectively short-circuits the system, saturating the amplifier. The same effect can be induced by forcing adherence to a curved surface without properly modifying the sensor to adjust the resting-state resistance.

3.2.2. Repeatability and Hysteresis

Surgical procedures often last for hours [71], and it is important that the system provide precise readings throughout. Under repeated identical conditions, the variance between readings are ideally as small as possible. FlexiForce sensor datasheet parameters indicate a repeatability of +/-2.5% [45], in a dry environment, with a flat active sensing area. Effects of curvature, as well as liquid environments must be experimentally investigated to determine any negative impacts on performance.

Repeatability experiments were also used to determine the feasibility of the calibration method. It should be noted that calibration on a curved surface is much more difficult than flat surface testing, due to center of mass shifting during deadweight application. It

is desirable to perform flat surface calibration, before curvature heat treatment, waterproofing, and instrument mounting.

Testing was performed on both flat surfaced sensors, as well as sensors subjected to curvature treatment as described earlier. The experimental procedures were as follows:

a. Clean sensor to remove irregularities from surface area

b. Secure sensor to test bench (flat bench surface, or cylindrical instrument)

c. Condition sensor (Apply and remove 150% of max load, cycle 3 times)

d. Apply force distribution puck

e. Apply increasing weights, record voltage

f. Remove all loads, allow system to stabilize.

A single sensor was tested 5 times using the same pressure increments, over the full pressure range. The testing time frame was approximately 30 minutes per experiment.

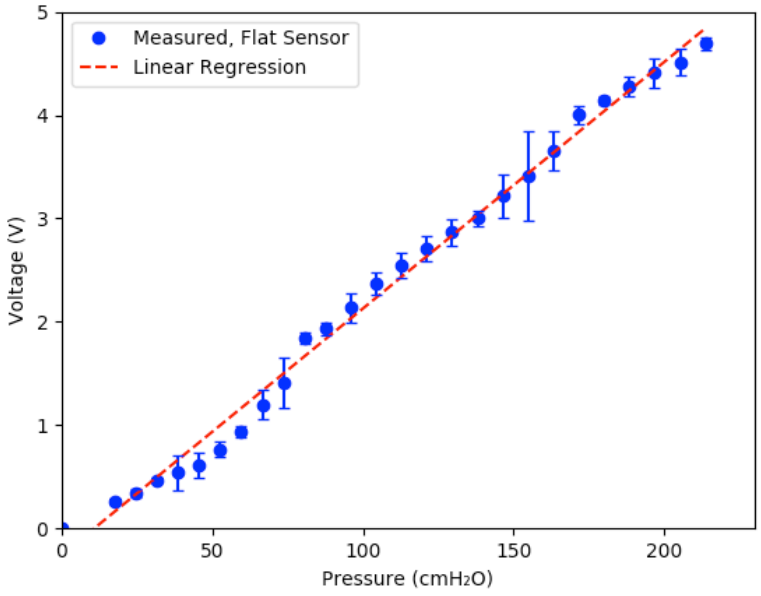

Figure 16: Repeatability testing. A factory condition, flat-surfaced sensor was subjected to 5 pressure trials over the FSO. Average standard deviation is ± .044V, for an error of 1.4% over the full range.

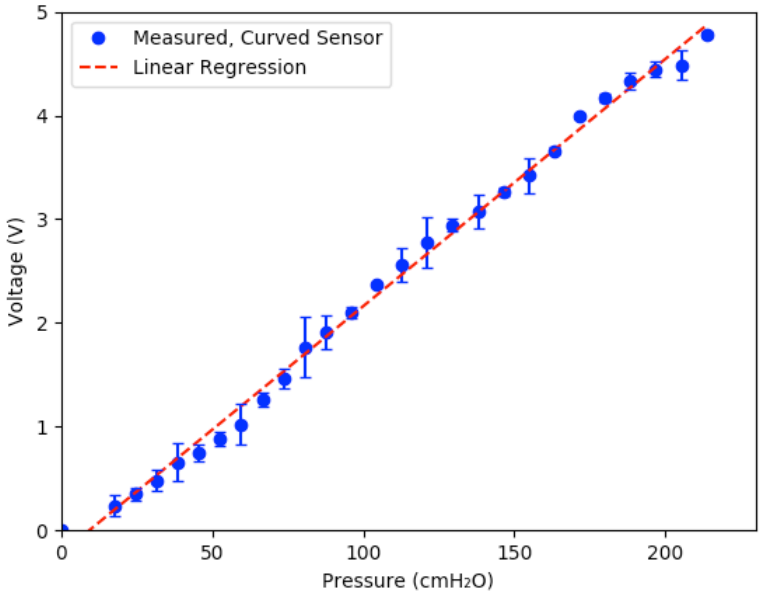

Figure 17: Repeatability testing results for a curved, instrument mounted sensor using 5 deadweight calibration trials. Average standard deviation ± .0365V, for a 1.1% error over the full range.

With dry testing repeatability testing completed, the waterproofed sensor was inserted into the water column, and sealed with silicone adhesive to prevent leakage around insertion point. The water column testing procedures are as follows:

1. Waterproof sensor with polyimide sleeve.
2. Affix sensor to instrument and verify resting state resistance.
3. Condition sensor (Apply and remove 150% of max load, cycle 3 times)
4. Insert instrument into water column and seal with silicone adhesive
5. Connect device to DAM and verify resting state resistance.
6. Pump liquid into the column, and tabulate voltages.
7. Disconnect sensor, and drain column.

Note that the resting state resistance is recorded several times to ensure that a leak has not occurred. A sudden drop in resistance can indicate that the waterproof seal has been compromised, leading to data corruption.

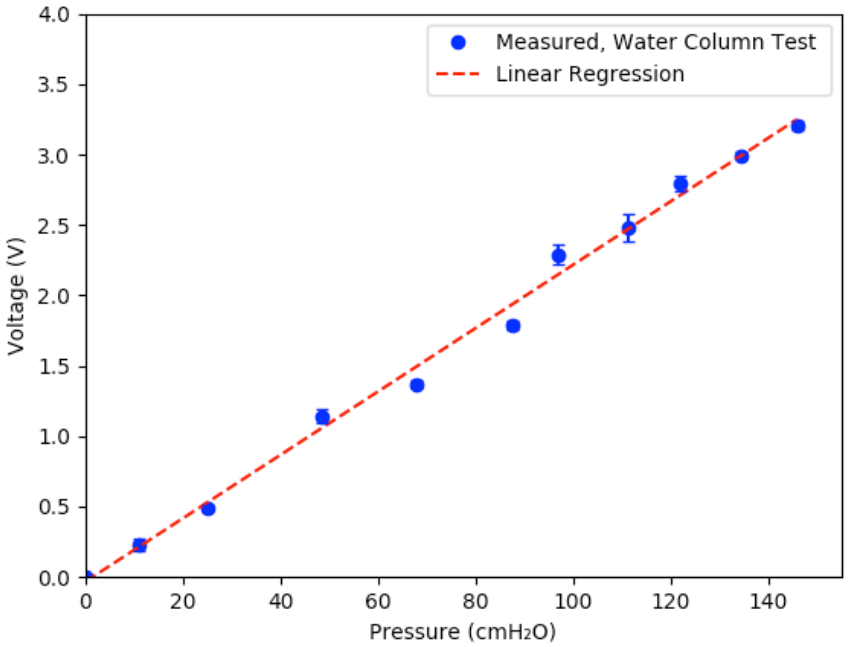

Figure 18: Repeatability testing results for a curved instrument mounted sensor for 5 water column calibration trials. Average standard deviation ± .0153V, with 2.5% error over full scale.

The data collected from each experiment is summarized in Table 2. The average standard deviation for flat (Fig. 16), mounted (Fig. 17), and liquid environment testing (Fig. 18) was found to be 0.0445 V, 0.0365 V, and 0.0153 V, respectively. Over the full scale, this translates to an error of 1.4%, 1.1%, and .5% respectively. The repeatability error decreases with the curvature, and then decreases again for the water column test. This may be due to hysteresis induced in the mounting process, which requires heating the substrate, and may affect piezoresistive qualities. In addition, the combination of both liquid and solid weights for the tests in figures 15 and 16 leaves the possibility of a slight

shift in center of mass as steel weights are added. This can shift the force distribution slightly and cause a greater variance between successive readings.

3.2.3 Reproducibility

The system is intended to be detachable and disposable, and sensors must be removable for instrument sanitization and disinfecting. When a new sensor is attached, it would be desirable to have very similar linear qualities, so that the linear regression calculated via calibration can be re-used. When the sensors are modified in the same manner to tightly conform to the instrument, the precision and accuracy of the system may be compromised. To determine the deviation of measurements, the performance of two separate sensors under the same test environment were analyzed. Two new sensors were conditioned on a flat surface by applying and removing 110% of the maximum load. Heat treatment to induce permanent curvature was applied to both, followed by waterproofing. Testing was performed in the water column, at a temperature of 20˚C. Experimental results are shown in Fig. 19.

Sensors that undergo identical characterization tests produce similar outputs. A difference of 1.86% in the linear fits (Fig. 19) indicates reasonable repeatability, and could possibly be mitigated by a more accurate calibration device such as a pressure gauge. Sensors were also prepared by hand, which present the possibility of inadvertent piezoresistive material damage by handling. If the reproducibility error between separate sensors is experimentally deemed as insignificant by the physician, identical prediction

models can be used without the need for a full calibration. The system can be relied on for accurate measurements, even with repeated usage or installment of a fresh sensor.

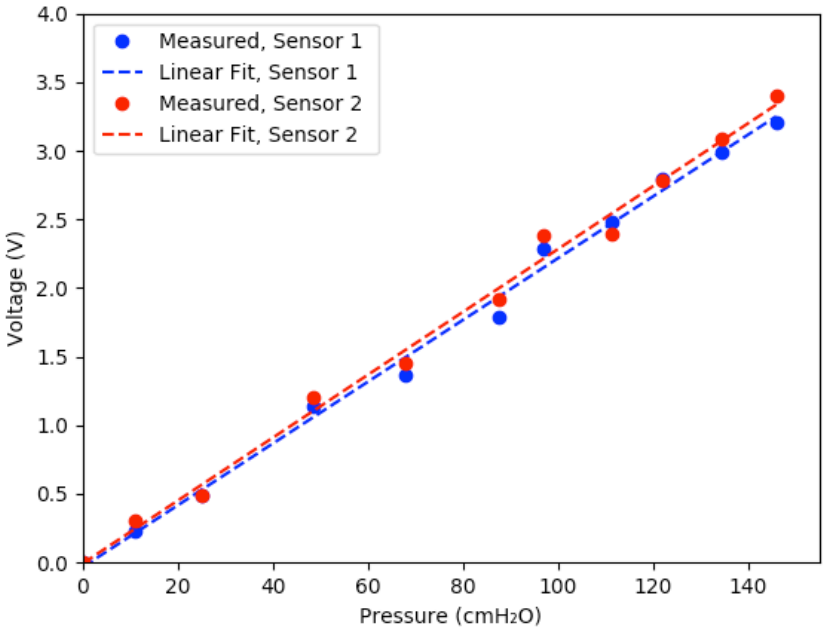

Figure 19: Reproducibility test results. Sensors were subjected the same calibration procedures, using identical pressure increments. Linear approximation is within 1.86 % of each other. Sensitivities for Sensor 1 and 2 are .02331 V/ cmH_20 and .02198 V/ cmH_20 respectively.

3.2.4 Linearity

The transfer function the electrical output signal is ideally linear for this application. Transfer functions for the sensor were obtained using the linear regression technique [72]. This technique is used to model the relationship between a dependent variable, and one or more explanatory variable. Water pressure is the only explanatory variable, with a *least squares* fit relating the measured data points. In this manner a predictive model can be formed to correlate physical pressure stimulus to electrical signals. Linear

approximation is implemented in Python, using the *NumPy.polyfit* function, the Python equivalent of Matlab's *polyfit* for linear regression calculations. The linearity is calculated as maximum deviation error from the slope of the line. A summary of linearity results is given in Table 2. Linear error increases slightly as modifications are made to the sensor, a possible side effect of wear-induced hysteresis. The coefficient of determination ($\boldsymbol{R^2}$), which is an indicator of prediction model accuracy in linear regression [73], is nearly 1 in all cases. This is a good indicator that the first-degree polynomial approximation model is suitable predictor.

The slope and offset of the best-fit line were used to construct the LabView data curve described in Section 2.2.3 in the form of $y = mx + b$.

Table 2: Linearity Characterization Summary

Experiment	Linearity	R^2	Slope	Offset
Flat sensor	1.7%	.996	41.61	11.5
Mounted Sensor (Dry)	1.3%	.998	41.79	9.6
Mounted Sensor 1 (Liquid)	2.6%	.997	44.18	1.8
Mounted Sensor 2 (Liquid)	2.7%	.996	43.37	0.75

3.2.5 Temperature Dependence

It is important to closely regulate the body temperature during an operation to prevent unintended perioperative hypothermia. Lowering of the body's core temperature to below 36.5˚C can be associated with increased morbidity and mortality [74]. Preventative measures are taken during surgery to avoid hypothermia, such as warming the patient with forced air warmers , or pre-warming fluids [75]. Most operating rooms are air-condition to keep the physician comfortable and alert, but can also chill intravenous fluids. Cold intravenous fluids such as saline and blood transfusions are usually warmed when large amounts are administered [76]. Other liquids utilized during surgery must also be regulated during surgery, and as a result the expected liquid-pressure operation temperature range will be limited.

Experiments were performed the effect of temperature changes on expected performance. Average air-conditioned room temperatures of 23 ˚C are assumed as the low end of the temperature spectrum, with a warmed irrigation liquid temperature of 37 ˚C as the high. The FlexiForce sensor indicates a change of up to 0.36% per ˚C, with greatest temperature-induced changes occurring above 74˚C, far above operating temperature.

An instrument-mounted sensor was placed horizontally through a section of clear vinyl tubing and sealed. Water was added to the tube such that the active sensing area was submersed in 2 cm of water. The water temperature start point was 23 ˚C, or room temperature, measured with infrared and alcohol thermometer. Cold water was removed

via syringe and replaced with warmer water, keeping the water column level to 2 cm. Results are shown in Fig. 20.

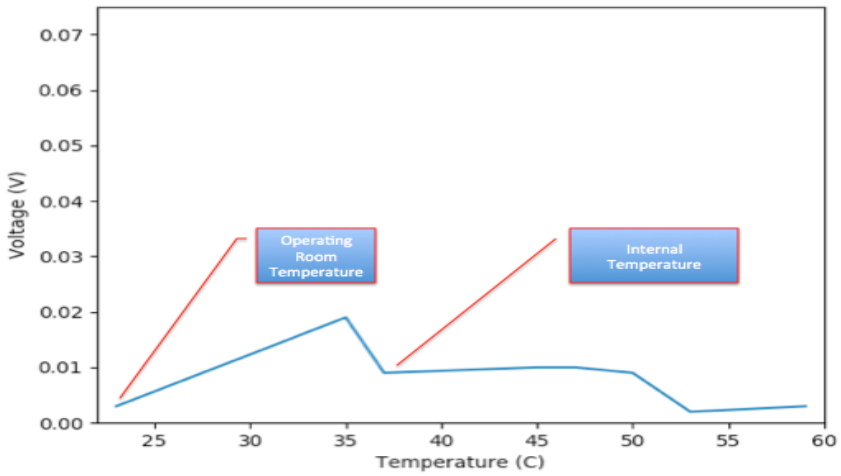

Figure 20: Temperature test results. Temperature range tested is from 23-59˚C, with average room temp and internal body temperatures indicated. Internal temperatures must be kept above 36.5˚ to avoid hypothermic complications.

A trend in the output is not apparent in this range, with a spike at 35˚ and a then a slight dip at 52˚. The difference between readings at room and internal temperatures is a miniscule 0.006V, translating to less than .18% error over full scale.

3.2.6 Characterization Summary

The performance characteristics are shown in Table 3. Wear on the sensor due to mounting, loading, and submersion does not seem to have much of an effect on the sensitivity, with only a .00039 V/ cmH_20 maximum difference between tests. A maximum of 1% difference in linearity is observed between best-fit lines.

Summation of the uncertainty across all tests (repeatability, reproducibility, linearity, temperature dependence) result in a **typical system error of ±4.5%** for a curved, waterproofed, instrument mounted sensor in a liquid environment.

Table 3: Characterization Summary

Experiment	Standard Deviation from Regression Slope (%err)	Average Standard Deviation	Sensitivity	Slope	Offset
Flat sensor (Figure 14)	.72 (1.7%)	±.0445	.02201 V/ cmH_20	41.756	11.5
Instrument mounted (Figure 15)	.55 (1.3%)	±.0365	.02237 V/ cmH_20	41.605	9.6
Water Column (Figure 16)	1.10 (2.6%)	±.0153	.021981 V/cmH_20	44.1817	1.8

5. Discussion

A typical error of 4.5% is relatively low for the proposed application. However, this value can possibly improved upon with more precise pressure measurement calibration equipment. The water column experiment was constructed to be a cost-effective solution to a liquid test environment. However, this method uses water column height markings, which introduces the possibility of clerical errors during transcribing. A calibrated pressure gauge attached at the same position as the pressure sensor can also be used as a known and accurate comparison standard. This is a more expensive solution, as pressure gauges capable of measuring below 1 psi are at least $500 USD.

It is difficult to quantify the damage to the sensor during the curvature-forming process. The polyester material of the sensor has a tendency to rebound to its normal flat state. To ensure a high resting-state resistance, the sensor must have a radius of curvature that is smaller than the instrument it is to be placed on. It was observed that even a very slight dent can render the piezoresistive material useless, while seemingly more severe wear had no effect. For example, one sensor was subjected to re-heating to correct the curvature four times, and when calibrated showed only a 1.9% difference in linearity compared to a fresh sensor. Conversely, a second sensor was peeled from an adhesive backing at a sharp angle, and was no longer usable. The sensing area is able to withstand much more wear if the encasing material is heated and allowed to relax. Sharp creases in any part of the sensing area will decrease resistance and drastically impact performance.

Based on the observed effects of wear, it is not recommended to use the same sensor more than once without a full recalibration. This effect could also possibly be worsened

by high-temperature sterilization, which will cause the substrate to relax and rebound to a flattened state.

Much of the uncertainty in sensor repeatability can be eliminated with a standardized and automated sensor fabrication procedure. This process could include assembling pre-curved sensors, so that the sensor need not have its geometry modified. The FlexiForce sensor is constructed of two layers of polyester, with a bonding adhesive between. During the drying process, the adhesive becomes porous, and susceptible to water seepage. A second sealant around the edges could waterproof the sensor, without the need for a polyimide sleeve.

The amount of data points used to construct the calibration curve of Fig. 17 to 19 is up to 26 individual points. Calibration need not be so rigorous, as fewer test points can be used to construct an accurate linear fit model as well. As shown in Table 2, the $\boldsymbol{R^2}$ value for a flat-surfaced sensor is exactly the same as an instrument-mounted sensor, whose curve was constructed with fewer points (26 and 10 respectively).

6. Conclusions and Future Work

A system to provide real-time liquid-pressure feedback could prove a very useful tool to a surgeon, especially one who does not yet have the experience necessary to spot potentially harmful pressure events. Even experienced surgeons can benefit from this system, as it can eliminate the distraction of constant monitoring. For the patient, a system such as this can possibly shorten recovery time, and ease an already strenuous experience.

This cost-effective system (less than $300) is a viable method of monitoring internal liquid pressures, without heavy instrumentation modification. Also appealing to a physician is that instruments they are comfortable and experienced with using need not be replaced by an entirely new system. The control interface is not difficult to learn, and should not provide much of a distraction while operating under safe pressure conditions.

A piezoresistive sensor such as the FlexiForce sensors characterized above could possibly have its performance improved by combining several other features. A pre-curved sensor would help mitigate modification errors. This could be accomplished by simply fixing the top polyester layer slightly wider than the bottom lamination, such that the adhesive could then prevent the layers from losing curvature. A waterproof edging, as well as a pre-bonded adhesive backing could create a simple and compact packaging that is easily stored, mounted, and discarded.

Another possible solution to the problem of damage-induced error is to create a sensor with a smaller active sensing area. A sensor whose width is much shorter than the diameter of the instrument will be much less affected by the curvature. This also expands the possible applications, as a wider range of instrument sizes can be used.

The system should also be tested in an actual surgical environment, so that unforeseen pitfalls can be evaluated. More physician feedback could also be helpful with the optimization of the user interface, providing the most intuitive and insightful interface possible. A solution as simple as this could satisfy the medical market need for a careful *in vivo* liquid pressure monitor, without a complete revamp of the instruments surgeons have experience using. The system has excellent potential for future clinical applications, and more importantly, the facilitation of a speedier recovery.

References

[1] Ellis, Harold. *A History of Surgery*. Cambridge University Press, 2002.

[2] Kirkup, J. R., "The history and evolution of surgical instruments." *Annals of the Royal College of Surgeons of England* 63.4 (1981): 279-285.

[3] Ackerknecht, Erwin H., and Lisa Haushofer. *A Short History of Medicine*. JHU Press, 2016.

[4] Berger, Darlene. "A brief history of medical diagnosis and the birth of the clinical laboratory. Part 1—Ancient times through the 19th century." *MLO Med Lab OBS* 31.7 (1999): 28-30.

[5] Burnett, John. "The origins of the electrocardiograph as a clinical instrument." *Medical History* Supplement 5 (1985): 53-76.

[6] McRobbie, Donald W., et al. *MRI from Picture to Proton*. Cambridge University Press, 2007.

[7] Vierra, M.D. Mark. "Minimally invasive surgery." *Annual Review of Medicine* 46.1 (1995): 147-158.

[8] Atroshi, Isam., et al. "Outcomes of endoscopic surgery compared with open surgery for carpal tunnel syndrome among employed patients: randomized controlled trial." *British Medical Journal* 332.7556 (2006): 1473-1481.

[9] Prodromakis, T., et al. "Biocompatible encapsulation of CMOS based chemical sensors." *IEEE Sensors, 2009*, Christchurch, New Zealand, 2009.

[10] "*In Vivo*." Def.1. *Merriam-Webster.com*. Merriam-Webster Dictionary Web. 1 July. 2017.

[11] Fearon, K. C. H., et al. "Enhanced recovery after surgery: a consensus review of clinical care for patients undergoing colonic resection." *Clinical Nutrition* 24.3 (2005): 466-477.

[12] Madhani, Akhil Jiten. "Design of teleoperated surgical instruments for minimally invasive surgery." Dissertation. Massachusetts Institute of Technology, 1998.

[13] Seibold, Ulrich., et al. "Prototype of instrument for minimally invasive surgery with 6-axis force sensing capability." *, 2005. ICRA 2005. Proceedings of the 2005 IEEE International Conference on Robotics and Automation*, Barcelona, Spain, 2005.

[14] Gafford, Joshua B., et al. "Microsurgical devices by pop-up book MEMS." *ASME 2013 International Design Engineering Technical Conferences and Computers and Information in Engineering Conference*, Portland, Oregon, 2013.

[15] Voelker, Rebecca. "Microsensor monitors eye pressure." *Journal of the American Medical Association* 315.15 (2016): 1555-1555.

[16] Ashruf, C. M. A. "Thin flexible pressure sensors." *Sensor Review* 22.4 (2002): 322-327.

[17] Pacchierotti, Claudio., et al. "Haptic feedback for microrobotics applications: a review." *Frontiers in Robotics and AI* 3.53 (2016): 1-7.

[18] Sonetha, Vaibhavi., et al. "Microelectromechanical systems in medicine." *Journal of Medical and Biological Engineering* 37.3 (2017): 1-22.

[19] Migliuolo, Michele, et al. "Medical and surgical devices with an integrated sensor." U.S. Patent Application No. 10/543,739.

[20] Kehlet, Henrik. "Surgical stress response: does endoscopic surgery confer an advantage?" *World Journal of Surgery* 23.8 (1999): 801-807.

[21] Tendick, Frank, et al. "Sensing and manipulation problems in endoscopic surgery: experiment, analysis, and observation." *Presence: Teleoperators & Virtual Environments* 2.1 (1993): 66-81.

[22] Tavakoli, Mahdi, R. V. Patel, and Mehrdad Moallem. "Haptic interaction in robot‐assisted endoscopic surgery: a sensorized end‐effector." *The International Journal of Medical Robotics and Computer Assisted Surgery* 1.2 (2005): 53-63.

[23] Meccariello, Giuseppe, et al. "An experimental study about haptic feedback in robotic surgery: may visual feedback substitute tactile feedback?" *Journal of Robotic Surgery* 10.1 (2016): 57-61.

[24] Leven, Joshua, et al. "DaVinci canvas: a telerobotic surgical system with integrated, robot-assisted, laparoscopic ultrasound capability." *Medical Image Computing and Computer-Assisted Intervention–MICCAI 2005* (2005): 811-818.

[25] Aron, Monish, et al. "Flexible robotics: a new paradigm." *Current Opinion in Urology* 17.3 (2007): 151-155.

[26] Holtz, David O., et al. "Endometrial cancer surgery costs: robot vs laparoscopy." *Journal of Minimally Invasive Gynecology* 17.4 (2010): 500-503.

[27] Kolata, Gina. "Results unproven, robotic surgery wins converts." *The New York Times,* 13 Feb. 2010.

[28] Brown, Malcolm, and J. E. A. Wickham. "The urethral pressure profile." *British Journal of Urology* 41.2 (1969): 211-217.

[29] Lose, Gunnar. "Urethral pressure measurements." *Acta Obstetricia et Gynecologica Scandinavica Supplement* 1.66 (1997): 39-42.

[30] Lopes, Marcel R., et al. "Goal-directed fluid management based on pulse pressure variation monitoring during high-risk surgery: a pilot randomized controlled trial." *Critical Care* 11.5 (2007): 1-9.

[31] Berguer, Ramon. "Surgical technology and the ergonomics of laparoscopic instruments." *Surgical Endoscopy* 12.5 (1998): 458-462.

[32] Lim, Jonas JB, and Arthur G. Erdman. "A review of mechanism used in laparoscopic surgical instruments." *Mechanism and Machine Theory* 38.11 (2003): 1133-1147.

[33] Roesthuis, Roy J., et al. "On using an array of fiber Bragg grating sensors for closed-loop control of flexible minimally invasive surgical instruments." *2013 IEEE/RSJ International Conference on Intelligent Robots and Systems,* Tokyo, Japan, 2013.

[34] Sung, Gyung Tak, and Inderbir S. Gill. "Robotic laparoscopic surgery: a comparison of the da Vinci and Zeus systems." *Urology* 58.6 (2001): 893-898.

[35] Green, Thomas H. "Urinary stress incontinence: differential diagnosis, pathophysiology, and management." *American Journal of Obstetrics and Gynecology* 122.3 (1975): 368-400.

[36] Vancaillie, Therry G., and William Scheusller. "Laparoscopic bladderneck suspension." *Journal of Laparoendoscopic Surgery* 1.3 (1991): 169-173.

[37] Kobashi, Kathleen C., et al. "Surgical treatment of female stress urinary incontinence: AUA/SUFU Guideline." *The Journal of Urology* 6.61 (2017): 1-9.

[38] Eriksen, Bjarne C., et al. "Long-term effectiveness of the Burch colposuspension in female urinary stress incontinence." *Acta obstetricia et gynecologica Scandinavica* 69.1 (1990): 45-50.

[39] Rogers, Rebecca G. "Urinary stress incontinence in women." *New England Journal of Medicine* 358.10 (2008): 1029-1036.

[40] Parker, William, Amy Rosenman, and Rachel Parker. *The Incontinence Solution: Answers for Women of All Ages*. Simon and Schuster, 2007.

[41] Albo, Michael E., et al. "Burch colposuspension versus fascial sling to reduce urinary stress incontinence." *New England Journal of Medicine* 356.21 (2007): 2143-2155.

[42] Robinson, John. "Fundamental principles of indwelling urinary catheter selection." *British Journal of Community Nursing* 9.7 (2004): 281-284

[43] Jocham, Dieter, et al. "Improved detection and treatment of bladder cancer using hexaminolevulinate imaging: a prospective, phase III multicenter study." *The Journal of Urology* 174.3 (2005): 862-866.

[44] Abboudi, Hamid, et al. "Learning curves for urological procedures: a systematic review." *BJU International* 114.4 (2014): 617-629.

[45] Tekscan, “Flexiforce A201 sensor datasheet.” FlexiForce A201 Datasheet, 2008.

[46] Wise, Kensall D., and James B. Angell. "An IC piezoresistive pressure sensor for biomedical instrumentation." *IEEE Transactions on Biomedical Engineering* 20.2 (1973): 101-109.

[47] Frobenius, Wolf D., Sanderson, A.C., and H. C. Nathanson. "A microminiature solid-state capacitive blood pressure transducer with improved sensitivity." *IEEE Transactions on Biomedical Engineering* 20.4 (1973): 312-314.

[48] Balavalad, Kirankumar B., and B. G. Sheeparamatti. "Design, simulation and analysis of a piezoresistive micro pressure sensor for pressure range of 0 to 1MPa." 2*016 International Conference on Electrical, Electronics, Communication, Computer and Optimization Techniques*, Mysuru, India, 2016.

[49] Puers, Robert. "Capacitive sensors: when and how to use them." *Sensors and Actuators A* 37-38 (1993): 93-105.

[50] Pritchard, Emily., et al. "Flexible capacitive sensors for high resolution pressure measurement." *IEEE Sensors, 2008*, Lecce, Italy, 2008.

[51] Grattan, K. T. V., and T. Sun. "Fiber optic sensor technology: an overview." *Sensors and Actuators A: Physical* 82.1 (2000): 40-61.

[52] Hollinger, Avrum, and Marcelo M. Wanderley. "Evaluation of commercial force-sensing resistors." *Proceedings of International Conference on New Interfaces for Musical Expression,* Paris, France, 2006.

[53] King, Chih-Hung, et al. "Tactile feedback induces reduced grasping force in robot-assisted surgery." *IEEE Transactions on Haptics* 2.2 (2009): 103-110.

[54] Priya, S. Krishna, A. N. Nithyaa, and R. Premkumar. "Screening of foot ulceration in diabetic neuropathy patients using FlexiForce sensor platform." *International. Journal of Science & Engineering Research* 5.4 (2014): 87-92.

[55] Mutoh, Tatsushi, et al. "Application of the FlexiForce contact surface force sensor to continuous extraocular compression monitoring during craniotomy for cerebral aneurysms." *Journal of Neurosurgical Anesthesiology* 22.1 (2010): 67-72.

[56] Kalantari, Masoud, et al. "A piezoresistive tactile sensor for tissue characterization during catheter‐based cardiac surgery." *The International Journal of Medical Robotics and Computer Assisted Surgery* 7.4 (2011): 431-440.

[57] Ferguson-Pell, Martin, Satsue Hagisawa, and Duncan Bain. "Evaluation of a sensor for low interface pressure applications." *Medical Engineering & Physics* 22.9 (2000): 657-663.

[58] Texas Instruments, *"*LM2917 frequency to voltage converter.*"* LM2917 Datasheet 2016.

[59] Das, Bhaba Priyo, Neville Watson, and Yonghe Liu. "Frequency-to-voltage conversion using OTA." *International Conference On Electronics and Information Engineering* Kyoto, Japan, 2010.

[60] National Semiconductors, "LM2917 - frequency to voltage converter data sheet." LM2917 Datasheet 2009.

[61] Brownrigg, D. R. K. "The weighted median filter." *Communications of the ACM* 27.8 (1984): 807-818.

[62] Perreault, Simon, and Patrick Hébert. "Median filtering in constant time." *IEEE Transactions on Image Processing* 16.9 (2007): 2389-2394.

[63] Mezher, Liqaa S., "Digital image processing filtering with LABVIEW." *International Journal of Computer Science Trends and Technology* 4.4 (2016): 278-282.

[64] Moore Jr, Alvin W., and James W. Jorgenson. "Median filtering for removal of low-frequency background drift." *Analytical Chemistry* 65.2 (1993): 188-191.

[65] "Calibration." Def.5. *Merriam-Webster.com*. Merriam Dictionaries, Aug. 2013. Web. 05 June. 2017.

[66] Young, Donald S., and Edward J. Huth, eds. *SI units for Clinical Measurement*. ACP Press, 1998.

[67] Kell, George S. "Density, thermal expansivity, and compressibility of liquid water from 0. deg. to 150. deg. correlations and tables for atmospheric pressure and saturation reviewed and expressed on 1968 temperature scale." *Journal of Chemical and Engineering Data* 20.1 (1975): 97-105.

[68] Wilson, Jon S. *Sensor Technology Handbook*. Elsevier, 2004.

[69] Gassmann, Eugen, "Pressure-sensor fundamentals: interpreting accuracy and error." *Chemical Engineering Progress* 110.6 (2014): 37-45.

[70] McKinney, Wes, *Python for Data Analysis: Data Wrangling with Pandas, NumPy, and IPython*. O'Reilly Media, Inc., 2012.

[71] Strum, David P., et al. "Modeling the uncertainty of surgical procedure times. Comparison of log-normal and normal models." *The Journal of the American Society of Anesthesiologists* 92.4 (2000): 1160-1167.

[72] Montgomery, Douglas C., et al. *Introduction to Linear Regression Analysis*. John Wiley & Sons, 2015.

[73] Nagelkerke, Nico JD. "A note on a general definition of the coefficient of determination." *Biometrika* 78.3 (1991): 691-692.

[74] Hart, Stuart R., et al. "Unintended perioperative hypothermia." *The Ochsner Journal* 11.3 (2011): 259-270.

[75] Hasegawa, Kenji, et al. "Core temperatures during major abdominal surgery in patients warmed with new circulating-water garment, forced-air warming, or carbon-fiber resistive-heating system." *Journal of Anesthesia* 26.2 (2012): 168-173.

[76] Mirza, Saqeb, et al. "The effects of irrigation fluid on core temperature in endoscopic urological surgery." *The Journal of Perioperative Practice* 17.10 (2007): 494.

[77] Brimacombe, Jill M., et al. "Effect of calibration method on Tekscan sensor accuracy." *Journal of Biomechanical Engineering* 131.3 (2009): 034503.